Basic Co-rich decagonal Al-Co-Ni: Superstructure

Angelica Strutz*
Laboratory of Crystallography, Department of Materials, ETH Zurich, 8093 Zurich, Switzerland

Akiji Yamamoto†
National Institute for Materials Science, Namiki 1, Tsukuba, Ibaraki 305-0044, Japan

Walter Steurer‡
Laboratory of Crystallography, Department of Materials, ETH Zurich, 8093 Zurich, Switzerland
(Received 25 May 2010; published 19 August 2010)

The four-layer superstructure of basic Co-rich decagonal $Al_{72.5}Co_{18.5}Ni_9$ was determined by single-crystal x-ray diffraction. Based on our previous work [A. Strutz, A. Yamamoto, and W. Steurer, Phys. Rev. B **80**, 184102 (2009)], a superstructure model was derived with five-dimensional (5D) noncentrosymmetric space-group symmetry $P\bar{1}02c$ with some additional constraints resulting from normal-mode analysis. The 5D structure model was refined with 250 parameters, resulting in values of $wR=0.039$ and $R=0.186$ for 1222 unique reflections. Its close relationship with the structure of W-Al-Co-Ni, a $\langle 3/2,2/1\rangle$ approximant, proves the physical validity of our structure model and justifies the use of the W phase for the derivation of structural principles underlying the formation of Al-based decagonal quasicrystals.

DOI: 10.1103/PhysRevB.82.064107 PACS number(s): 61.05.cp, 61.44.Br, 61.50.Ah, 61.66.Dk

I. INTRODUCTION

This is part II of our structure analysis of basic Co-rich decagonal $Al_{72.5}Co_{18.5}Ni_9$ (d-Al-Co-Ni). In part I,[1] we described the determination of the two-layer average structure while here in part II we present the solution of the actual four-layer superstructure. This is the first determination of such a superstructure, which is quite common in aluminum-based decagonal quasicrystals. In the system Al-Co-Ni, the lateral correlation length of the superstructure decreases with decreasing Co/Ni ratio by approximately two orders of magnitude while it remains constantly large along the periodic direction. Basic Co-rich d-Al-Co-Ni is the only decagonal quasicrystal modification that has sharp superstructure reflections related to the four-layer periodicity, allowing a quantitative structure analysis. All others show only diffuse scattering phenomena which get weaker and less peaked and structured with increasing Ni content, being no more observable at all in case of basic Ni-rich d-$Al_{70.2}Co_{5.4}Ni_{24.4}$.[2–4]

The formation of a twofold superstructure along the periodic direction stabilizes all low-temperature modifications of d-Al-Co-Ni and all their approximants with the exception of the Ni-rich ones.[2] At high temperatures, the entropic contribution, mainly by Co/Ni disorder and vacancy formation, is sufficient for the stabilization of these phases and all superstructures disappear. In order to better understand formation, stability, and physical properties of d-Al-Co-Ni full structural information, not only averaged one, is required. More than 500 papers on these phases and structurally related d-Al-Co-Cu and d-Al-Fe-Ni testify the broad interest in these model systems justifying the tedious determination of the superstructure.

One of the main results of the determination of the average structure in part I was that it allows the direct derivation of the two layer average structure of the W phase, a high rational approximant of d-Al-Co-Ni, by a five-dimensional (5D) shear operation. And one of the goals of the determination of the superstructure of d-Al-Co-Ni was to find out whether this is also true for the full four-layer structure of the W phase. In this case, the W phase can be employed as a periodic model system, suitable for quantum-mechanical calculations, for all modifications of d-Al-Co-Ni as well as d-Al-Co-Cu and d-Al-Fe-Ni. Furthermore, its fundamental building clusters can be used for modeling the structures of all modifications of these decagonal phases. That this works has already been demonstrated.[5]

For the experimental details concerning the single-crystal x-ray diffraction data collection and reduction see part I. There, we already pointed out that the $h_5=2n$ reciprocal space layers, containing main reflections only, resemble those of the basic Ni-rich phase, while those with $h_5=2n+1$, containing superstructure reflections only, can be only indexed employing the superstructure basis. Depending on the value of $m=(\Sigma_{i=1}^{4}h_i) mod\ 5$, we can distinguish between main reflections ($m=0$) and superstructure reflections of first (S1, $|m|=1$) and second order (S2, $|m|=2$). The intensities of S1 reflections are systematically stronger than those of S2 reflections as it is usually the case for first- and second-order satellites.

The superstructure basis is identical to that of the superstructure of type I,[6] which is related to that of the basic structure by rotoscaling, i.e., a rotation by $\pi/10$ and scaling by a factor of $1/[2\cos(\pi/10)]=0.5257$. This leads to the quasilattice parameter $a_s=5.221(4)$ Å and the period $c_s=8.144(2)$ Å along the tenfold axis. According to the determinant of the transformation matrix,[7] basic Co-rich d-Al-Co-Ni is a fivefold superstructure (regarding the volume of the 5D unit cell) of the basic Ni-rich modification in the quasiperiodic directions and a twofold one along the tenfold axis. Both types of superstructures have been analyzed in the work presented here.

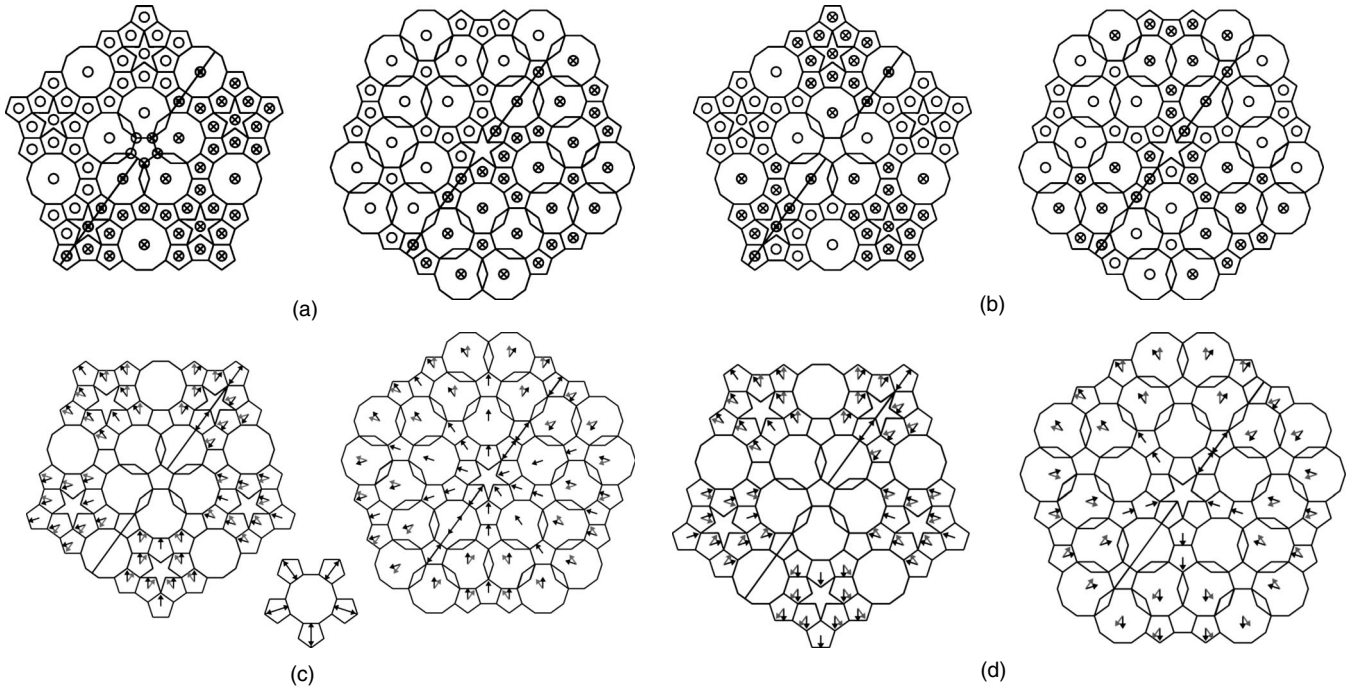

FIG. 1. Different shift modes generating the superstructure. [(a) and (b)] Atoms in the puckered layer at $x_3=1/8$ can be displaced along the periodic direction. Empty (crossed) circles mark shifts into the [0 0 1 0 0], up ([0 0 $\bar{1}$ 0 0], down) direction. [(c) and (d)] Atoms in the flat layer at $x_3=3/8$ can have shifts only within the quasiperiodic layer. Note: although the arrows are plotted in the respective subdomains they denote shifts that are only in external space.

II. 5D STRUCTURE MODEL BUILDING

For d-Al-Ni-Fe, a similar peculiar distribution of main and superstructure reflections as in our case has been observed and qualitatively explained by a 5D structure model with color symmetry.[8] Unfortunately, this approach is not applicable to our case since it lacks the necessary degrees of freedom for the description of puckered quasiperiodic atomic layers. We need these degrees of freedom because we know from the structure of the W phase that at least two of the four quasiperiodic layers have to be puckered. We also know from the diffraction pattern that the superstructure reflections do not systematically decay with increasing values of h_5, indicating that the atomic displacements along the tenfold axis strongly contribute to the intensities of the superstructure reflections.

A hard constraint for our superstructure model is set by symmetry. According to the 5D space group $P\bar{1}02c$, the occupation domain (OD) in the layers separated by one half of the translation period are related by the c-glide operation cutting them into halves (OD transformed by the c-glide operation will be marked by primed symbols); OD A and A′ as well as B and B′ are, additionally, related by reflection on the mirror plane perpendicular to the tenfold direction and halfway between them (note: $\bar{1}0=5/m$).

Another hard constraint is that the projection of the actual four-layer structure onto the two-layer period has to reproduce exactly the average structure determined in part I. This means that we can neither change the general shapes of the five ODs A, B,C, D, and E [see part I and Fig. 1 of supplementary material (Ref. 9)] nor those of their small subdomains. If we denote the OD of the average structure by the subscript $_{AS}$, we get the following conditions: $A_{AS}=A+A'$, $B_{AS}=B+B'$, $C_{AS}=C+C'$, $D_{AS}=D+D'$, and $E_{AS}=E+E'$. This means that in projection the point symmetry of all OD has to be $\bar{1}0m2$. At contrast, in the actual superstructure the fivefold symmetry of the OD is broken and the point symmetry is reduced to m for OD C, D, C′, and D′, which are located within mirror planes and are generating flat atomic layers, and that of OD A, A′, B, and B′, generating puckered atomic layers, is even lowered to 1.

The relationships between the symmetry of the average structure and that of the superstructure, together with the above-mentioned peculiar reciprocal-space distribution of main (even) and superstructure reflections (odd reciprocal-space layers), put strong constraints on the allowed shifts and chemical occupancies of the subdomains. Unfortunately, because of the very limited number of observable superstructure reflections, not all remaining allowed parameters can be refined. Therefore, starting from the average structure described in part I, we constrain in our superstructure model the relevant parameters in the form of shift and substitutional modes obtained from a symmetry-based normal-mode analysis. Four different shift modes and two substitutional modes, symmetric and antisymmetric ones, were selected and used simultaneously in the refinements.

The shift modes are realized by different combinations of the external space shifts u_1, u_2, and u_3 for each subdomain. Shifts u_3, i.e., along the periodic axis [0 0 0 0 0 ± 1] are only allowed for OD A and B, which generate the puckered atomic layers. For these OD, two different shift modes were used as shown in Figs. 1(a) and 1(b). Empty circles and

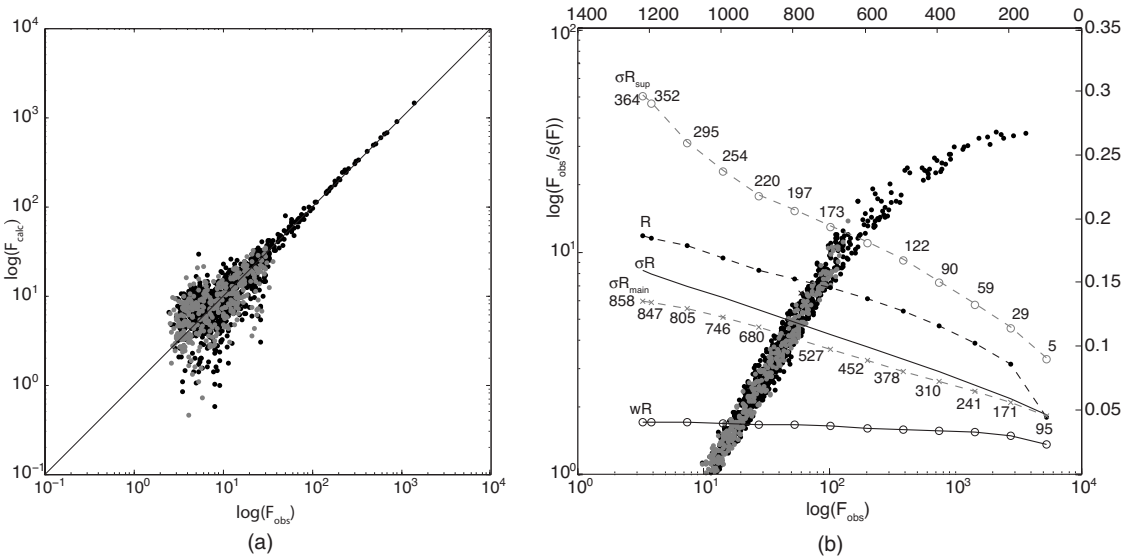

FIG. 2. (a) F_{obs}/F_{calc} plot for the final model of $Al_{72.5}Co_{18.5}Ni_9$. The 858 main and 364 superstructure reflections are marked as black and gray dots, respectively. (b) Distribution of F_{obs}/σ_F on a double-logarithmic scale for main and superstructure reflections (black and gray dots, respectively). Weighted, unweighted, and expected R factors (right scale) as a function of the N strongest reflections (top scale). The expected R factors, σR, are given as function of the N strongest reflections with N given at the respective data points.

crossed circles identify subdomains with displacement vectors [0 0 0 0 0+1] (up) and [0 0 0 0 0−1] (down), respectively. For these OD, the reflection conditions do not allow displacements parallel to the quasiperiodic layers. The maximal amplitude of ≈0.5 Å was observed for the subdomains 47, 52–55. These subdomains are fully occupied by Al.

At contrast, OD C and D, located within mirror planes and generating the flat atomic layers, have displacements within the quasiperiodic layers only. The two different shift modes employed are shown in Figs. 1(c) and 1(d) with external space shift directions indicated by arrows. Atoms originating from the outermost subdomains 168, 169, 184, 185, 200, 201, 210–213 experience large shifts exceeding 1 Å. Therefore their total occupancies were set to one half. In the external space, these atoms are located in the decagonal cages of the 20 Å clusters. The comparison with the 20 Å clusters in the W phase reveals similar atomic relaxations in the quasiperiodic flat layers, mainly due to the presence of vacancies.

The two substitutional modes are of the same type as shown in Figs. 1(a) and 1(b) but only apply to OD C and D. The symbols mark now plus and minus deviation of the Al/TM (transition metal) occupancy from equal distribution. The variations in the Al/TM occupancies, in most of the cases, are coupled with the displacements parallel to the quasiperiodic layers. Analysis of the changes in R factors during the refinement shows that the importance of the substitutional modes in the superstructure formation is less significant in comparison with puckering or with displacements parallel to the quasiperiodic layers. The maximal amplitude of the total substitutional modes of ≈50% was observed for

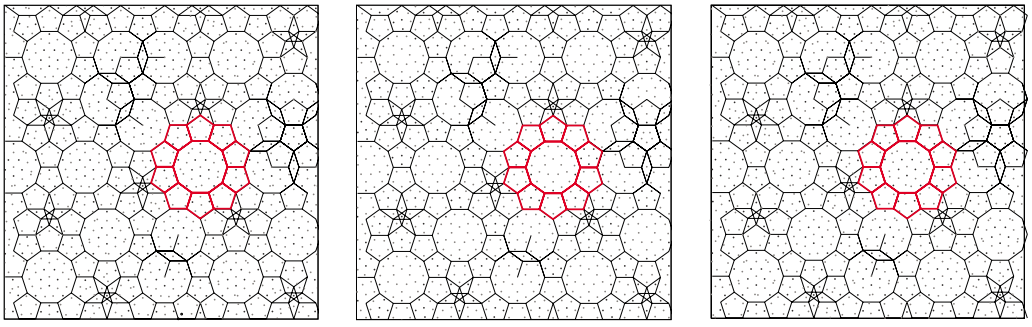

FIG. 3. (Color online) 70×70 Å^2 sections of the atomic layers at (a) $x_3=-1/8$ (flat), (b) $x_3=1/8$ (puckered), and (c) $x_3=3/8$ (flat) of the four-layer superstructure of decagonal $Al_{72.5}Co_{18.5}Ni_9$. The two flat layers, located on mirror planes, are related by a c-glide plane in the 5D structure. White and black circles correspond to Al and TM atoms, respectively. The thick (online red) outlined ≈20 Å cluster can be compared with Fig. 5 in part I. There, the average structure layer at $x_3=3/4$ [part I Fig. 5(a)] corresponds to the superposition of the superstructure layers at (a) $x_3=3/8$ and (c) $x_3=7/8$, and that at $x_3=1/4$ [part I Fig. 5(b)] to the superposition of the superstructure layers at (b) $x_3=1/8$ and $x_3=5/8$. The structures are related by a $\pi/10$ rotation around [00100].

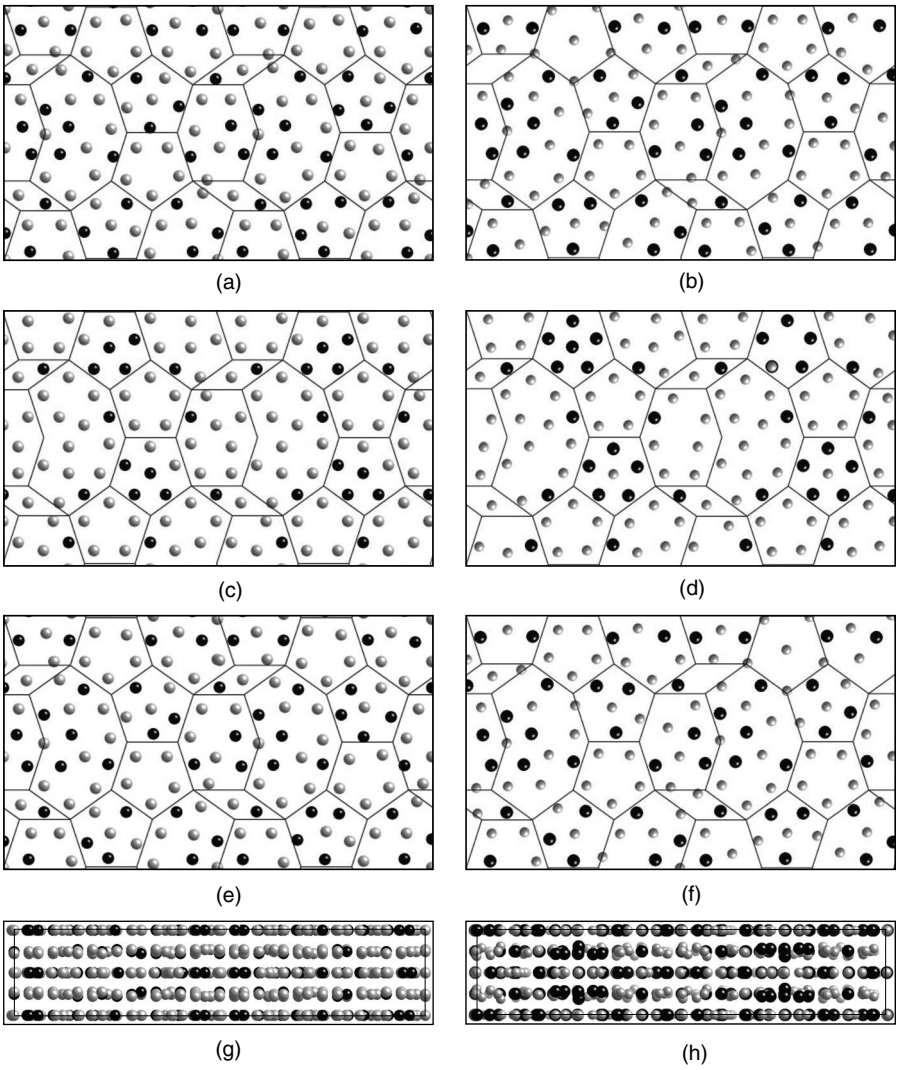

FIG. 4. Layers of the W phase as derived from [(a), (c), (e), and (g)] basic Co-rich d-$Al_{72.5}Co_{18.5}Ni_9$ compared to its actual structure [(b), (d), (f), and (h)] (Ref. 13); [(a) and (b)] flat $x_3=3/8$, [(c) and (d)] puckered $x_3=1/8$, [(e) and (f)] flat $x_3=-1/8$, and [(g) and (h)] the layer structure shown along x_3. Gray and black circles correspond to Al and TM atoms, respectively.

the subdomains 160, 161, 190–193 related by a fivefold symmetry.

III. STRUCTURE REFINEMENT

All structure refinements have been performed using the program package QUASI07_08.[10] In the first step, one scale factor and two parameters for secondary extinction correction as well as all average structure parameters[1] were refined against the full data set. These parameters include: for each OD the overall external[11] space atomic displacement parameters (ADPs), $B_{\|}$ within the quasiperiodic plane and $B_{\perp}$ perpendicular to it ($B=8\pi^2\langle u^2\rangle$ with u the displacement amplitude); for each subdomain the external space shifts u_1, u_2 from the ideal positions as defined by the coordinates of the respective OD and the Al/TM site occupancy (mixing parameter s_1). The limited number of reflections does not allow to refine individual ADP for each subdomain.

In the next step, the superstructure parameters were successively refined in addition. As in the superstructure the fivefold symmetry of the OD is broken, the number of symmetrically independent subdomains is drastically increased from 53 in the average structure to 275. This is more than just $5\times53=265$, because the subdomains cut by the c-glide plane have to be split into two parts. In order to keep the number of parameters as small as possible, all shifts less than their standard deviations were reset to zero and fixed in the further refinement steps.

In addition, a phason displacement parameter was refined to $b^i=0.684(2)$ Å^2. A penalty function was included in order to constrain the chemical composition, which then was refined to $Al_{72.3}TM_{27.7}$ compared to the actual one of $Al_{72.5}TM_{27.5}$. Since the standard deviations of our data were calculated from averaging up to 40 symmetrically equivalent reflections, they are systematically underestimated with regard to systematic errors (weak intensity data integration, for instance). For the minimization of the weighted reliability factor, wR, we used weights directly proportional to the standard deviations,[12] consequently.

The refinement of the 250 parameters (therefrom 117 superstructure parameters) against the 1222 unique reflections with $|F_o|>1\sigma(|F_o|)$ converged to $wR=0.039$ and $R=0.186$. The reliability factors for the 858 main reflections amount to $wR=0.034$, $R=0.150$, those for the 364 satellite reflections to $wR=0.405$ and $R=0.364$. For a list of the resulting refined parameters see Table 1 of supplementary material.[9]

The quality of the least-squares fit is reflected in the F_{obs}/F_{calc} distribution shown in Fig. 2(a). It clearly shows that the fit of the weak superstructure reflections is of the same quality as that of the main reflections. The rather high R factor for the superstructure reflections can be attributed mainly to their weak intensities leading to large standard deviations and problems for intensity integration. Multiple diffraction effects may also contribute. The internal R factors, resulting from the averaging of symmetrically equivalent reflections, indicate the range where the refinement R factors are expected to be. In our case, R_{int} values of 0.422 and 0.591 have been obtained for superstructure reflections of type S1 and S2, respectively.

The distribution of F_{obs}/σ_F for main (black dots) and superstructure (gray dots) reflections [Fig. 2(b)] shows perfect coincidence. This means, that statistical and systematic errors are equally distributed for both reflection classes. In the same figure, the dependence of reliability factors on the number of reflections used for their calculation is shown in comparison with the expected R factor, $\sigma R=\Sigma\sigma_F/\Sigma|F_{obs}|$. This reliability factor corresponds to the unweighted R factor if $\Delta=|F_{obs}|-|F_{clc}|=\sigma_F$. Usually, due to systematic errors, Δ is significantly larger. The expected R factors are: for all reflections $\sigma R=0.159$, for main reflections $\sigma R_{main}=0.135$, and for superstructure reflections $\sigma R_{sup}=0.296$.

The maxima and minima of the residual electron density according to the difference Fourier maps in external space are $\Delta\rho^e_{max}=0.86\ e\text{Å}^{-3}$ and $\Delta\rho^e_{min}=-0.87\ e\text{Å}^{-3}$, respectively. The corresponding values for the maxima and the minima of the full electron density are $\rho^e_{max}=43.54\ e\text{Å}^{-3}$ and $\rho^e_{min}=-6.12\ e\text{Å}^{-3}$, respectively. Electron density maps calculated by the maximum-entropy method agree with the structure derived from the 5D model.

IV. 3D STRUCTURE MODEL AND THE W PHASE

A three-dimensional (3D) structure model in physical space can be obtained by a proper irrational cut of the refined 5D structure model. Three successive atomic layers are shown in Fig. 3. The most prominent difference between the superstructure and average structure is the presence of puckered layers (at $x_3=1/8$ and 5/8) in the former. The maximum puckering amplitudes amount to ± 0.5 Å, comparable to those in the W phase. In the flat layers (at $x_3=3/8$ and 7/8), the shifts for some atoms reach values of up to 1.4 Å. There are no too short distances resulting between fully occupied atomic positions, only between half-occupied atomic split sites.

To check the physical relevance of the obtained structure model, we generated its $\langle 3/2,2/1\rangle$ approximant with lattice parameters $a^{av}_{app}=19.884$ Å, $b^{av}_{app}=8.1425$ Å, and $c^{av}_{app}=23.375$ Å as described in part I. Figure 4 shows a comparison of three different layers of the W phase constructed from the 5D model of the quasicrystal with the actual experimentally obtained structure.[13] With the exception of a few atomic sites, the agreement is surprisingly good. Surprisingly, because a really existing approximant (W phase) needs not to be a perfect rational approximant. To summarize, the four-layer superstructure is mainly caused by a puckering of every other layer and a relaxation of the flat layers in between. These building principles are also found in the other approximants in the system Al-Co-Ni.[2]

V. CONCLUSIONS

Since real quasicrystals are never strictly quasiperiodically ordered, diffraction experiments can only give a kind of globally averaged 5D structure model. In our case of a tenfold superstructure, the limited observable diffraction data set limits the complexity and information content of the resulting structure model. Therefore, we see as the main result of this first quantitative structure analysis of the four-layer superstructure of d-Al-Co-Ni that the W phase is a good rational approximant, indeed. This gives the clue for the modeling of all the different modifications of aluminum-based decagonal phases with four-layer period since the clusters identified in the W phase can be used as fundamental clusters for this purpose.[5] Furthermore, the results of the first-principles calculations performed for the W phase can be transferred to some extent to the decagonal phase.[13] Then, the ordering phenomena as a function of the Co/Ni ratio can be related to the TM atomic environments that significantly differ in the case of Ni and Co atoms, respectively.

*angelica.strutz@mat.ethz.ch
†yamamoto.akiji@nims.go.jp
‡steurer@mat.ethz.ch

[1] A. Strutz, A. Yamamoto, and W. Steurer, Phys. Rev. B **80**, 184102 (2009).
[2] W. Steurer, Z. Kristallogr. **219**, 391 (2004), and references therein.
[3] S. Katrych and W. Steurer, Z. Kristallogr. **219**, 606 (2004).
[4] W. Steurer and S. Deloudi, *Crystallography of Quasicrystals: Concepts, Methods and Structures*, Springer Series in Materials Science Vol. 126 (Springer-Verlag, Berlin, 2009).
[5] S. Deloudi, F. Fleischer, and W. Steurer (unpublished).
[6] K. Edagawa, M. Ichihara, K. Suzuki, and S. Takeuchi, Philos. Mag. Lett. **66**, 19 (1992).
[7] A. Yamamoto, H. Takakura, and E. Abe, Phys. Rev. B **72**, 144202 (2005).
[8] A. Yamamoto and S. Weber, Phys. Rev. Lett. **79**, 861 (1997).
[9] See supplementary material at http://link.aps.org/supplemental/10.1103/PhysRevB.82.064107 for an overview of OD and their subdomains as well as the list of all parameters.
[10] A. Yamamoto, Sci. Technol. Adv. Mater. **9**, 013001 (2008).
[11] Where necessary, external (physical or parallel) and internal (perpendicular) space parameters are marked by superscripts *e* or *i*, respectively.
[12] W. Massa, *Crystal Structure Determination* (Springer-Verlag, Berlin, 2004), p. 117.
[13] K. H. Hassdenteufel, A. R. Oganov, S. Katrych, and W. Steurer, Phys. Rev. B **75**, 144115 (2007), and references cited therein.